www.ijarp.com ISSN 2456-9992 Page: 01-13

International Journal Advanced Research Publications

Research Article

Volume: 02
Issue: 02

FACTORIAL ANALYSIS OF STREAM SEDIMENTS: CONOSCOPIC VIEW FOR BARIUM AND REE MINERALISATION IN AND AROUND SAMAPLATI AREA, TAMIL NADU

***Vishnu Kumar Singh**

India.

Article Received: 02 January 2026, Article Revised: 22 January 2026, Published on: 10 February 2026

***Corresponding Author: Vishnu Kumar Singh**

India.

DOI: https://doi-doi.org/101555/ijarp.1296

ABSTRACT

The study area falls under southern granulite terrain bounded by two curvilinear shear zones and part of Salem block . geologically the area composed of 3 group of rocks, they are 1) Older metamorphic group consists of Dunite / Peridotite, meta pyroxenite and meta gabbro rocks, 2) The Charnockinte Group consists of magnetite quartzite, pyroxene granulite and charnockite rocks and 3) The migmatite group consists of hornblende biotite gneiss, pink and grey granitic gneiss. Gabbro/dolerite dykes are younger basic intrusives and pegmatite / quartz veins are younger acid intrusives intruded in to the country rock. The data of stream sediments includes concentrations (in ppm) of 16 trace elements: Ba, Ga, Sc, V, Th, Pb, Ni, Co, Rb, Sr, Y, Zr, Nb, Cr, Cu, and Zn, measured using XRF method. Enrichment factors (EF = sample concentration / UCC value) were calculated. Values >1 indicate enrichment relative to UCC, >2 suggest moderate enrichment, and >10 indicate significant anomaly, potentially indicating ore-forming processes Maximum EF >10: Ba (max ~35x in sample 68), Sr (~7x, but not >10), Zr (~11x in sample 101), Nb (~7x), Cr (~13x in sample 15), Cu (~10.9x in sample 26), Zn (~2.5x). . High variability in Ba, Sr, Zr, Cr, and Cu suggests localized enrichment processes, possibly related to mineralization.by PCA analysis of samples PC1 (~30-40% variance): High loadings on mafic elements (Sc 0.3, V 0.3, Ni 0.3, Co 0.3, Cr 0.3, Cu 0.2, Zn 0.2), representing mafic component.PC2 (~20-30% variance): High loadings on incompatible elements (Ba 0.3, Rb 0.3, Th 0.2, Y 0.2, Zr 0.3, Nb 0.3), representing felsic/granitic component. Cluster analysis reveals three main groups: background, Ba-rich (felsic), and Cr-Ni rich (mafic). PCA highlights mafic vs felsic controls on variance, while t-SNE visualizes distinct distributions.

INTRODUCTION:

Primary and secondary dispersion/halo of elements can bring out the concealed deposit of economical consideration , this study will prove how geochemical and multivariate statistical techniques will decipher the REE and barium enrichment of economical grade in the study area .Samalpatti alkaline -carbonatite complex falls in the south-eastern part of toposheet . Ultramafics such as dunite, pyroxenite and different types of syenite and carbonatite represent the alkaline complex emplaced during neoproterozoic. Dunite occurs as discrete isolated bodies within pyroxenite. The contact is sharp. Pink syenite veinations within dunite are seen near Yeddarapatti and Pokkampatti.. Alkali pyroxenite occurs as discontinuous semi circular arcuate bodies on the peripheral part of the Samalpatti complex and the younger syenite and carbonatite veins cut across the pyroxenite. Pyroxenite exposures are seen around Nattam, Sunnampatti, Kanjanur and SE of Samalpatti. The syenite complex is seen between Sunnampatti - Tippampatti in the north and Kolalpatti in the south extending in a NE - SW direction over a length of 6.5 km and width of about 5 km. Based on the colour, composition, grain size and textural variation, more than a dozen varieties of syenite have been recognised., riebeckite syenite veins,barite- carbonate veins and aplitic syenites. Carbonatite occurs as intrusives within the pyroxenite and adjoining gneisses. The intricate network of carbonatite vein activity in the pyroxenite is seen around Salamarathupatti and Mettusulakkarai, Six types of carbonatites (texture & composition)viz., dark grey, greenish whitish grey, brownish grey, white (epidote bearing) and pure white soviet type have been recognized. Pyrochlore ,apatite and allanite were the primary phases of REE enrichment in the area . High value of Barium (Ba) values (>1000ppm) were observed in many soil samples, maximum value being 22,322 ppm in grid No.68. high value of Ba is also reflected in C3-R(26,453ppm. High value of Ce is observed in sample no 68(3385.29ppm), 69(1957.67ppm), 54(1019ppm), 55(904ppm) and 42(1135ppm). High value of Ce is also observed in R and C sample; C3-R(2893.8ppm), C3 C(2561.02ppm), and C2-R (1172.02ppm). The total LREE's varies from 68.62 ppm to 7702.3 ppm and total HREE's varies from 3.11 ppm to 46.31 . multivariate statistics plays a vital role to decipher the origin & distribution of barium and REE minerals . geochemical data of stream sediments and techniques such as PCA,tSNE and cluster analysis narrow down the possibility of Barium and Rare earth elements mineralization

METHODOLOGY

Major oxides, Cr, Rb, Sr, Y, Zr, Nb, Ba, Ga, Sc, V, Th, Pb, Ni, Co, Cu and Zn were analysed

by XRF (Make and Model: Malvern Panalytical; Axios mAX4KW WD-XRF Spectrometer). REE's, As, Sn, In, Hf, Ta, U were analysed by ICPMS (Make and Model: ICPMS - Agilent make, 7700X). Standard reference material GSD and GSS series, IGGE China with known element concentrations was analysed after each batch of 20 samples for accuracy and duplicate samples after each batch of 10 samples was analysed for repeatability. In addition, repeated analysis of 5% of stream sediment samples were carried out to validate unambiguously the consistency in sampling and the accuracy in the analytical procedures.

GEOLOGICAL ARCHITECTURE OF THE STUDY AREA

The mapped area forms a part of southern granulite terrain (SGT) of Precambrian age. The geology of the area composed of 3 group of rocks, they are 1) Older metamorphic group consists of Dunite / Peridotite, meta pyroxenite and meta gabbro rocks, 2) The Charnockinte Group consists of magnetite quartzite, pyroxene granulite and charnockite rocks and 3) The migmatitic group consists of hornblende biotite gneiss, pink and grey granitic gneiss. Gabbro/dolerite dykes are younger basic intrusives and pegmatite / quartz veins are younger acid intrusives intruded in to the country rock. Pyroxene granulite also occurs as 2 to 5 m wide and 0.2 to 1.5 km long linear folded bands in close association with magnetite quartzite with the migmatite gneiss. These are exposed near Jambukuttapatti, Pattanur, 1.5 km east of Amman koil patti and around Kanganeri. Charnockite shows gradational contact with the enveloping migmatite gneiss and epidote hornblende gneiss. Major charnockite areas are seen near Jumbukattapatti, Pochampalli and Attipalayam areas. Pyroxenite, occurs as rafts and linear bands within charnockite. Major bodies of pyroxenite are seen around Sandur, Kureampatti, Kuchchanur, Pochampalli and 1km NNW of Chettiyur.Banded biotite gneiss is the predominant gneissic rock and occupies a major area in the west and south-eastern parts. This mesocratic rock is distinctly different from the epidote hornblende gneiss and the migmatite gneiss. This rock type is well exposed around Tippampatti, Salur and Mattur river course. The granitoids gneiss, which is another variety of gneiss in gneissic complex occupies the north central part and also occurs as bands within the banded biotite gneiss in the northwestern part. Grey migmatite is the result of migmatisation of pre-existing granulites. Well-developed agmatitic structures are seen near Kariyampatti, Gajalnayakkanpatti and Kappalavadi. Epidote hornblende gneiss is exposed in the southern, southeastern and eastern parts. Earlier this was considered as fenite. However, recent studies indicate that epidote hornblende is the hydrothermally retrograded product of the pre-existing granulite and high-grade gneiss. Epidote is seen as thin veinlets and profuse diffusions. Effects of shearing are well observed.

Epidote and pink feldspar venations are common. Good exposures are seen around Mettusulakkarai, Bajjanur, Pemmalkuppam, Ampalli and Kullampatti. A major WNW - ESE to NW – SE trending dyke system is seen in the northern part. In the southern segment comparatively, smaller dykes are emplaced along NNE - SSW to ENE - WSW directions. Most of the dykes are dolerite in composition. The WNW - ESE trending dykes in the northern part run for several kilometers along their strike.

The famous Samalpatti alkaline -carbonatite complex falls in the southeastern part. Ultramafics such as Dunite, pyroxenite and different types of syenite and carbonatite represent the alkaline complex emplaced during neoproterozoic. Dunite occurs as discrete isolated bodies within pyroxenite. The contact is sharp. Pink syenite veinations within dunite are seen near Yeddarapatti and Pokkampatti. Magnesite venations and suspentinisation are observed in Kanjanur hill. Formation of calcrete is commonly observed. Alkali pyroxenite occurs as discontinuous semi circular arcuate bodies on the peripheral part of the Samalpatti Complex and the younger syenite and carbonatite veins cut across the pyroxenite. Pyroxenite exposures are seen around Nattam, Sunnampatti, Kanjanur and SE of Samalpatti. The syenite complex is seen between Sunnampatti - Tippampatti in the north and Olapatti and Kolalpatti in the south extending in a NE - SW direction over a length of 6.5 km and width of about 5 km. Based on the color, composition, grain size and textural variation, more than a dozen varieties of syenite have been recognised. Leucocratic homophanous syenite is the major type. Other types are white syenite, fine grey syenite, coarse grey syenite, whitish grey garnet syenite, medium grey hornblende syenite, coarse leuco hornblende syenite, pale pinkish white syenite, grey porphyritic syenite, pink syenite, pink porphyritic syenite, pegmatoidal syenite, riebeckite syenite veins, falcite and aplitic syenites. Carbonatite occurs as intrusives within the pyroxenite and adjoining gneisses. The intricate network of carbonatite vein activity in the pyroxenite is seen around Salamarathupatti and Mettusulakkarai, where pyroxenes were altered to talc, chlorite, phlogopite, serpentine and asbestos. Six types of carbonatites viz., dark grey, greenish, whitish grey, brownish grey, white (epidote bearing) and pure white soviet type have been recognized.

Minor unmappable quartz and pegmatite veins traverse the gneissic terrain. The NNE extension of the Harur - Uttangarai quartz vein zone is marked by floats of vein quartz in the southeastern corner. The Charnockite Group of rocks exhibit granulite facies meta morphism. Different phases of migmatisation had retrograded the granulites to amphibolite facies grade. Development of carbonated gneiss is seen in the vicinity of carbonatite intrusions. The popular dimension stone 'Paradiso' is being quarried near Mallukal, Chandanur, Sadanaykhanpatti and

Pungampatti. Pockets of vermiculite are seen at several places around Kanjanur.

RESULT & DISCUSSION

Stream sediments carry the signature of rocks presents in the study area only the elements in excess would reflect in the stream sediments. Enrichment factors (EF = sample concentration / UCC value) were calculated. Values >1 indicate enrichment relative to UCC, >2 suggest moderate enrichment, and >10 indicate significant anomaly, potentially indicating ore-forming processes or specific lithologies. Mean EF across elements, most elements have mean EF ~1-3, indicating overall similar to UCC, but with outliers. Mean EF >2: Ba (~1.5-2, but skewed by outliers), Sr (~1.8), Zr (~3), Nb (~1.8), Cu (~1.1), Zn (~0.75).Low EF: Ni (~0.8), Co (~0.7), Cr (~1.2), suggesting depletion in some mafic elements. Maximum EF >10: Ba (max ~35x in sample 68), Sr (~7x, but not >10), Zr (~11x in sample 101), Nb (~7x), Cr (~13x in sample 15), Cu (~10.9x in sample 26), Zn (~2.5x). Ba is highly enriched in samples 24,37,38,40,42,53,54,55,68,69 (EF >10, up to 35x), possibly indicating barite or feldspar-rich zones' enriched in samples 1,30,60,71,102,105,115,159 (EF >8, up to 11x), suggesting zircon accumulation or granitic rocks' highly enriched in samples 12,51,52,59,64,79,114 (EF >10, up to 59x in sample 51), indicating chromite or ultramafic influence's in samples 26,83 (EF >10), possibly sulphide mineralization. Other elements like Ni in sample 51 (EF ~10), Th in some (max ~3.8x).

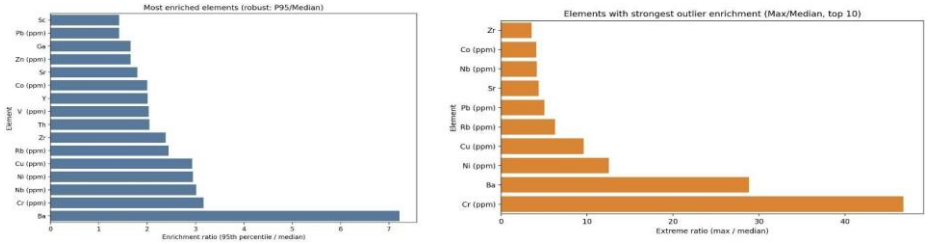

Figure 1: enrichment histogram of trace elements. (toposheet no 57L/7)

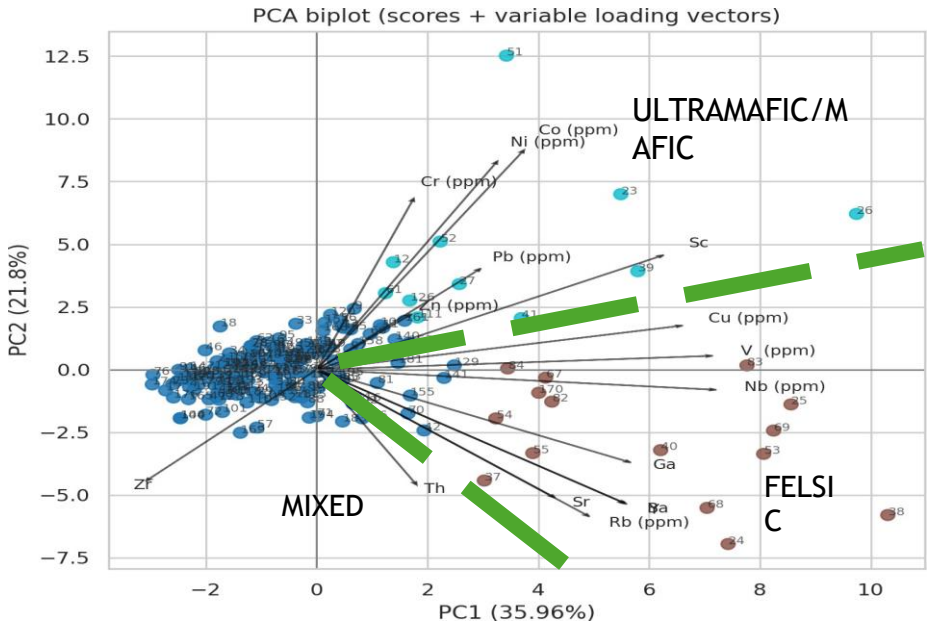

Figure 2: elemental distribution of sample point over principal components plane.

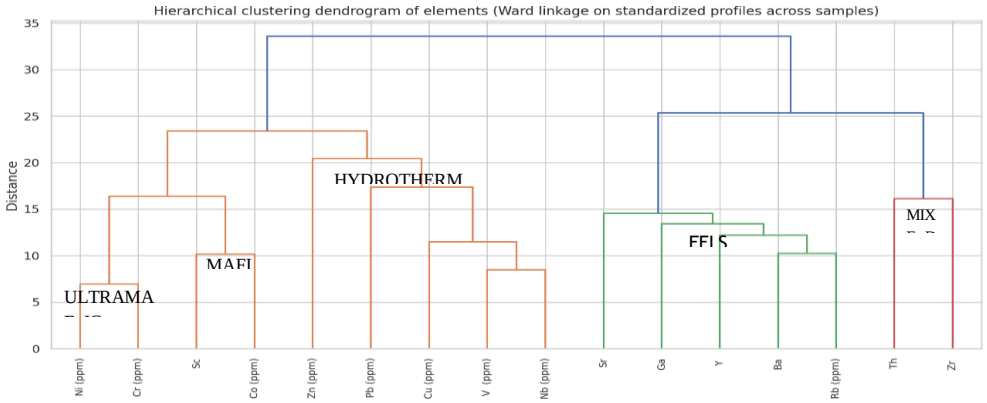

Figure 3: Dendogram (ward linkage) depicting origin of elemental concentration in the stream sediments.

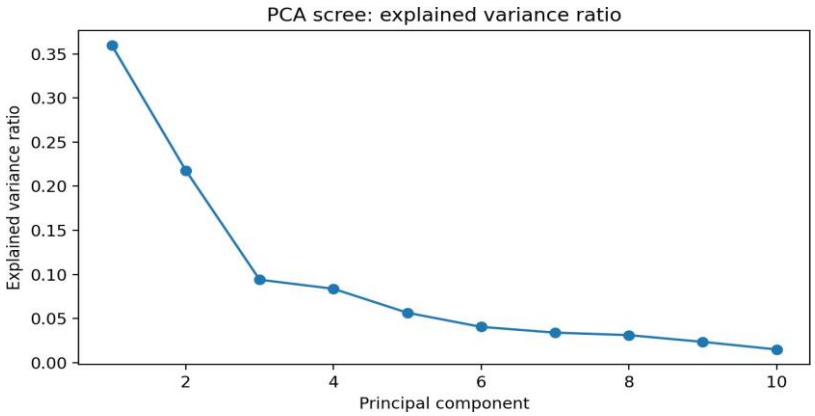

Figure 4: scree plot of principal components showing relative loading of components (Different source rocks have different loadings)

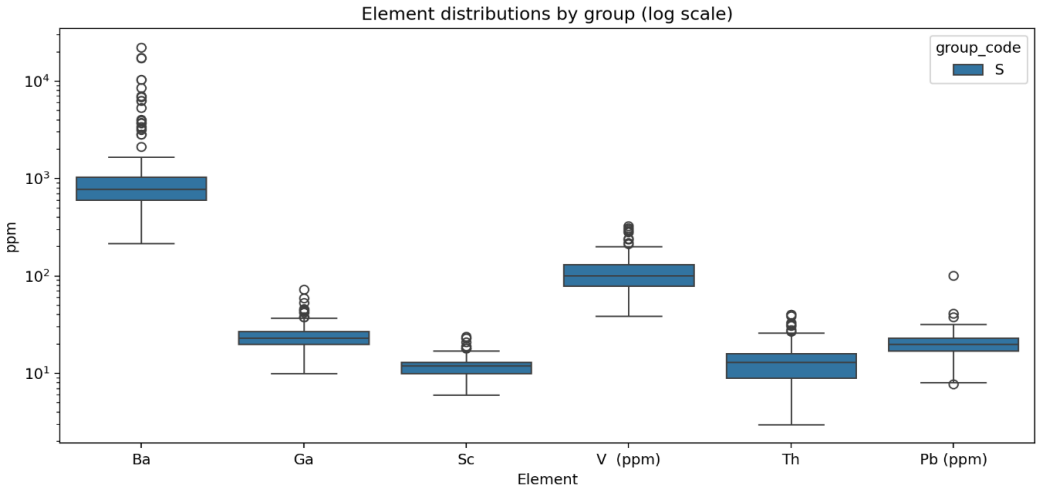

Figure 5: Barium shows maximum outlier points in whisker plots (probably mineralization in the study area)

Case for REE enrichment or mineralization

The average TREE is 450.44 ppm (~0.45 ppm), which is below typical crustal averages but shows significant variability (standard deviation of 698.17 ppm). The median (264.70 ppm) is lower than the mean, indicating a right-skewed distribution with a few high-concentration outliers suggesting potential mineralization hotspots.

Element Dominance Light REEs (LREEs: La, Ce, Pr, Nd) dominate, comprising ~90% of TREE on average. Ce is the most abundant (mean 198 ppm), followed by La (113 ppm) and Nd (79 ppm). Heavy REEs (HREEs: Tb-Lu) are much lower, with means below 5 ppm each.

LREE vs. HREE Partitioning

REEs are often categorized into LREEs (La, Ce, Pr, Nd, Sm, Eu, Gd) and HREEs (Tb, Dy, Ho, Er, Tm, Yb, Lu) to assess fractionation patterns, which can indicate mineralization types (e.g., carbonatite-related deposits are LREE-enriched).

Statistics	Mean	STD dev	Min	25%	50%	75%	Max
LREE	438.37	693.97	68.62	182.62	254.74	441.19	7702.3
HREE	12.07	6.03	3.13	8.54	10.26	13.45	46.31
LREE/HREE	32.05	22.9	9.63	19.79	24.83	34.33	166.32

Patterns: The dataset is strongly LREE-enriched (mean LREE/HREE = 32.05), typical of many REE deposits like monazite or bastnäsite-bearing systems. HREE fractions are low, suggesting limited heavy REE mineralization. The high max ratio (166.32) in one sample indicates extreme LREE dominance, possibly from a highly fractionated source.

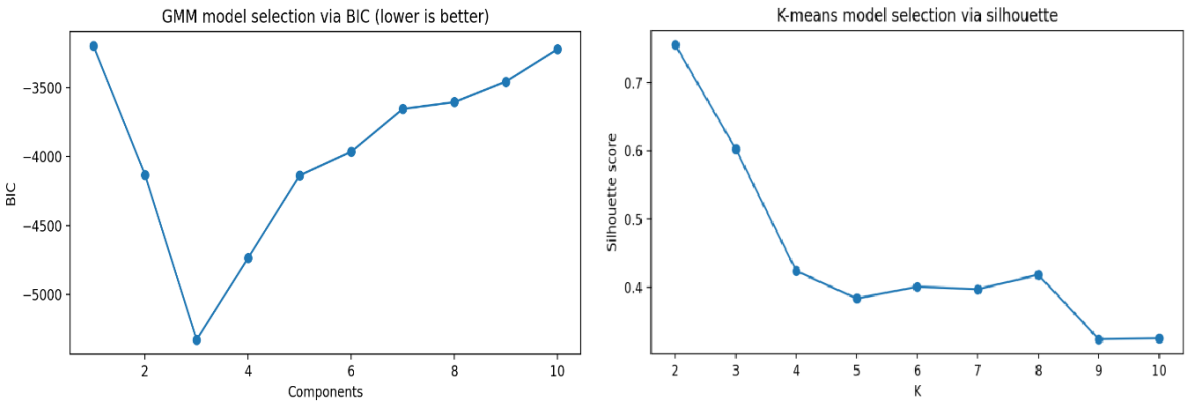

Fig 6: sample clustering by K mean for REE mineralization or anomaly.

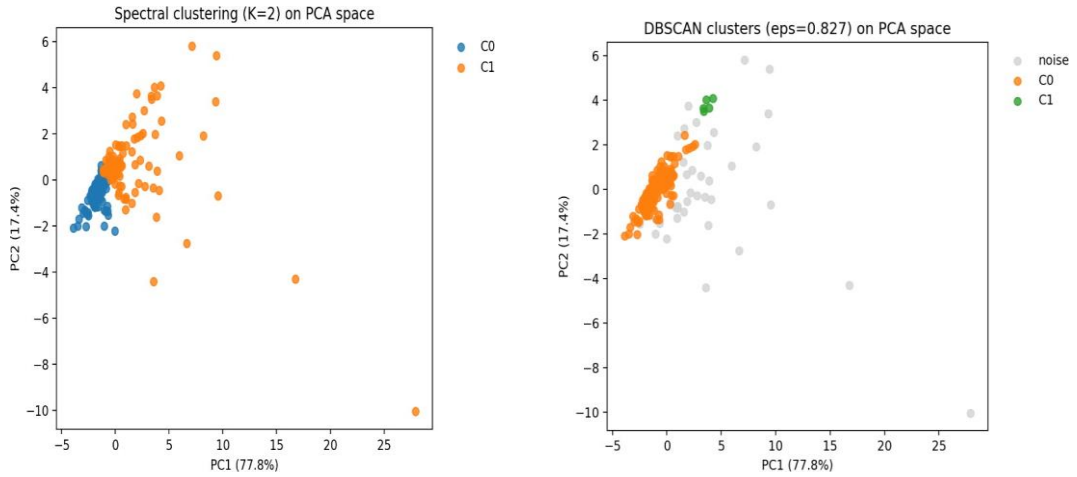

Figure 7: spectral clustering of sample on PC space (theme REE mineralization)

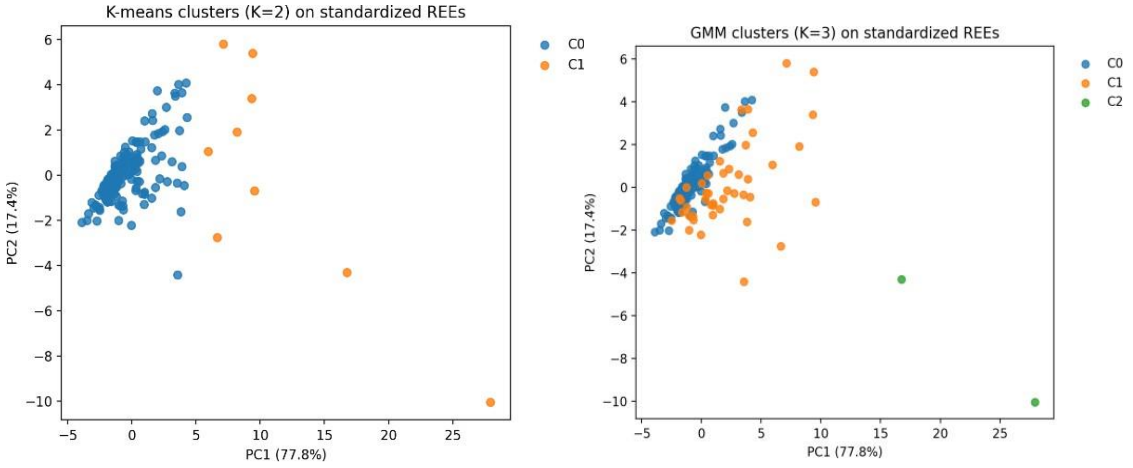

Figure 8: K mean clustering of stream sediments and their distribution on principle component space.

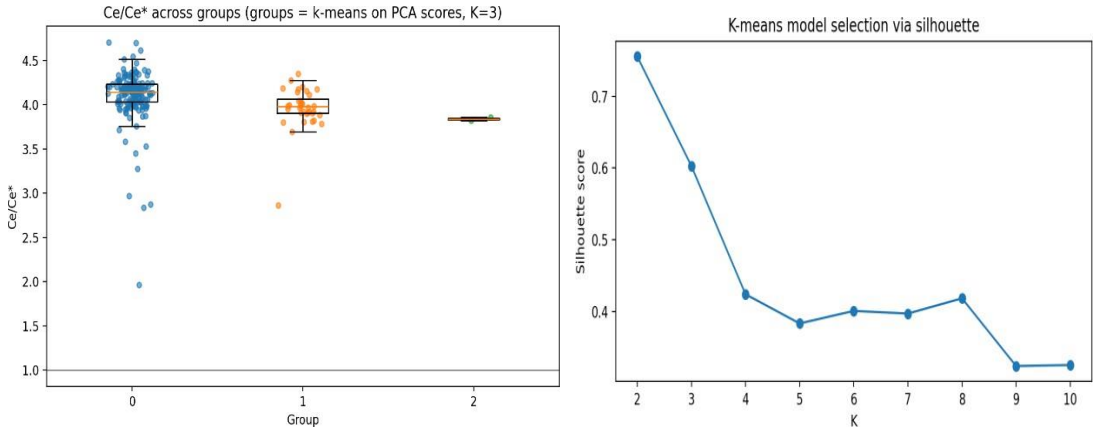

Figure 9: Different clustering plots for stream sediments on PC space.

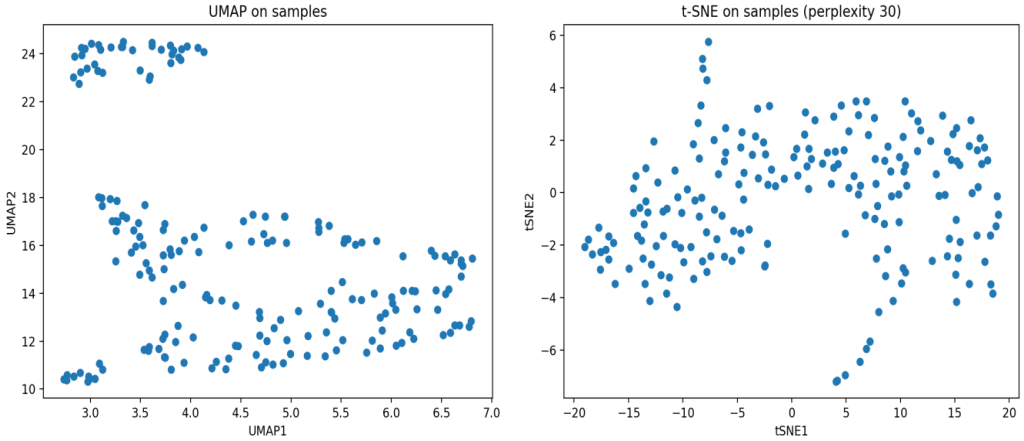

Figure 10: UMAP and tSNE to understand the variability between samples on principle component space.

Distribution and Variability

TREE Distribution: Most samples (75%) have TREE < 456 ppm, with a cluster around 200–300 ppm. However, the distribution is skewed by outliers: ~10% exceed 500 ppm, and 5% exceed 1,000 ppm. This suggests background levels in many samples, with sporadic elevated concentrations indicative of mineralization.

Outliers and Anomalies: A boxplot analysis reveals several high outliers (e.g., >1,000 ppm), which could represent mineralized zones. The histogram shows a unimodal distribution with a long tail toward higher values.

Correlations: TREE correlates strongly with LREEs (e.g., Ce: 0.999, La: 0.998), confirming LREE control. HREEs show weaker correlations (e.g., Dy: 0.752), reinforcing the LREE bias. Eu anomalies (potential redox indicators) are present but mild (mean Eu: 2.22 ppm).

Samples with High Mineralization Potential

Samples with TREE >1,000 ppm (arbitrary threshold for "elevated" based on dataset; ~2x

mean) may indicate significant mineralization. Here are the top 10 by TREE . These top samples account for ~30% of the total TREE sum across the dataset, highlighting concentrated mineralization in a subset.

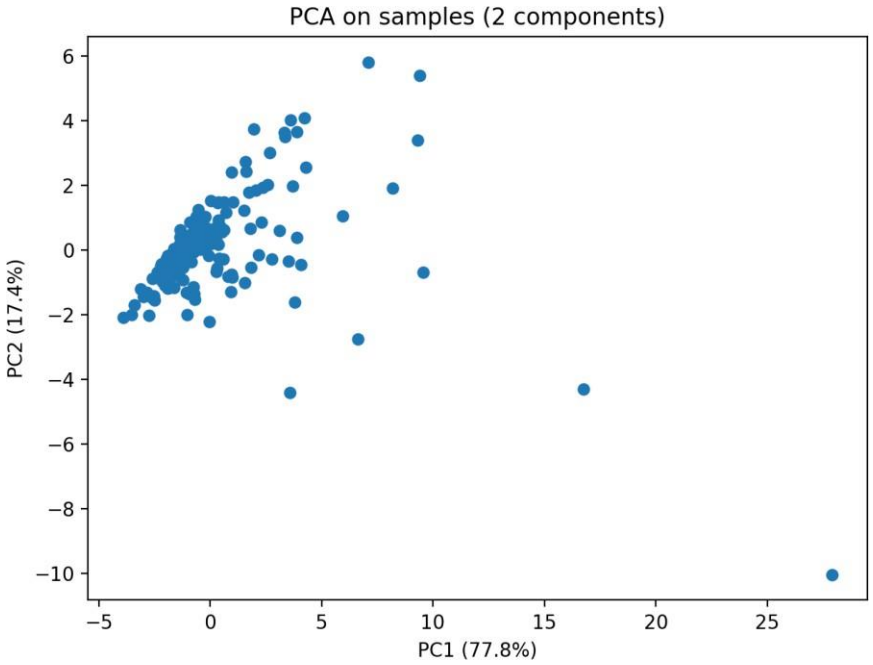

Figure 11: Distribution of stream sediments on PC1 vs PC2 space (to understand variability and outlier behaviour between samples)

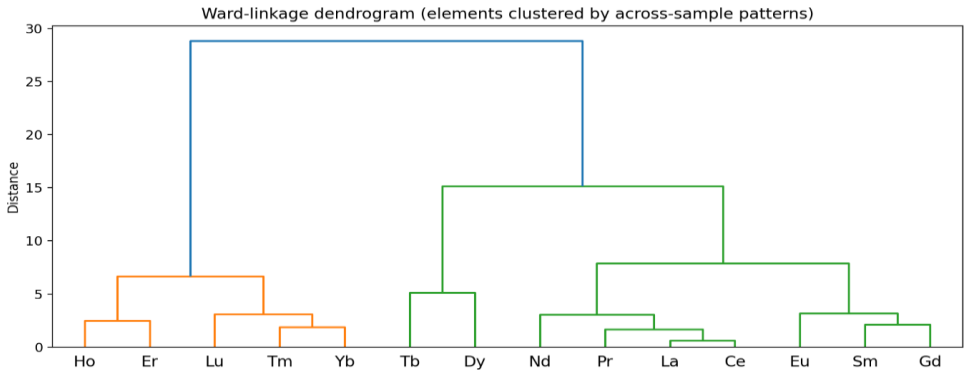

Figure 12: ward linkage between samples in form of elements depicts the different origin and enrichment.

Factor analysis (a type of factorial analysis) was performed on the provided REE dataset to identify underlying patterns in mineralization. This statistical method reduces dimensionality and reveals latent factors explaining variance in REE concentrations, which can indicate geochemical processes (e.g., fractionation in magmatic or hydrothermal systems). The data was standardized to account for differing scales, and 3 factors were extracted using maximum

likelihood estimation. Results show high communalities (variance explained by factors) for most elements (>0.90), indicating a good fit.

Proportion of total variance accounted for by each factor (cumulative: 96.1%).

Factor	Proportion
Factor 1	0.705
Factor 2	0.208
Factor 3	0.047

Interpretation in Context of Mineralization

-Factor 1 (70.5% variance)**: Strongly loads on light REEs (LREEs: La, Ce, Pr, Nd, Sm, Gd, Eu >0.96). This represents overall REE abundance and LREE enrichment, common in carbonatite or alkaline deposits where bastnäsite or monazite dominate. High values suggest samples with bulk mineralization (e.g., outliers like row 69 with TREE 7748 ppb).

- Factor 2 (20.8% variance): Positive for heavy REEs (HREEs: Tm, Yb, Lu, Er, Ho, Dy >0.48), negative/mild for LREEs. This captures LREE/HREE fractionation, possibly due to fluid evolution or mineral partitioning (e.g., in xenotime-rich zones). In barium-associated systems, this could relate to sulfate complexing affecting HREE mobility.

Factor 3 (4.7% variance): Loads on heaviest HREEs (Lu, Yb, Tm >0.34) with negative Eu. This may indicate Eu anomalies (redox-sensitive) or specific late-stage mineralization, as seen in some manganese-hosted REEs with barium

CONCLUSION

(i) Implications for Barium & REE Mineralization

Enrichment Patterns: The data suggests Barium and LREE-dominated mineralization, possibly linked to alkaline igneous / carbonatite systems common in REE deposits. Low HREE indicates limited potential for high-value heavy REEs

(ii) Different statistical techniques point out three possible origins for Barium and REE mineralization in the study area.

(iii)Here Factor 1 represent (70.5% variance) and also the possible reason for REE and Ba mineralization.

REFERENCES:

1. Balaram, V. (2019). Rare earth elements: A review of applications, occurrence, exploration, analysis, recycling, and environmental impact. *Geoscience Frontiers*, 10(4), 1285-1303. (Discusses REE mineralogy, deposits like bastnäsite and monazite, and oceanic ferromanganese crusts with REE concentrations.)
2. Odom, W.E., Doctor, D.H., McAleer, R.J., Benton, J.R., Gray, A.A., & Pitts, A.D. (2025). Rare Earth Element (REE), Critical Mineral, and Geochemical Characterization of Manganese Oxide Ore Deposits in the Virginia Piedmont and Valley & Ridge. U.S. Geological Survey data release. https://doi.org/10.5066/P13WA9AS. (Highlights barium enrichment (median 12,480 ppm) in manganese oxide ores alongside REEs in Appalachian deposits.)
3. Li, C., Xu, G., Guo, X., Ling, X., & Wu, B. (2024). The Origin and Evolution of Rare Earth Element Mineralization in the Muluozhai Deposit (Sichuan, China): Insightsfrom Mineralogical, Trace Element, and Sr-Nd-Pb-C-O-Ca Isotope Data. *EconomicGeology*, 119(3), 681-706. (Examines barite-celestine in carbonatite-hosted REE veins, with barium's role in fractionation and mantle-derived fluids.)
4. Weng, Q., Niu, H.C., Qu, P., et al. (2022). Mineralization of the Bayan Obo rare earth element deposit by recrystallization and decarbonation. *Economic Geology*, 117, 1327-1338. (Focuses on REE-Nb-Fe genesis in the world's largest REE deposit, with implications for associated minerals like barite.)
5. Dos Santos, E.C., de Andrade, L.A., & de Lima, R.M.F. (2025). Rare Earth Elements: A Review of Primary Sources, Applications, Business Investment, and Characterization Techniques. *Applied Sciences*, 15(20), 10949. (Reviews major REE minerals like monazite and bastnäsite, with examples from Bayan Obo and corporate mining activities.)
6. Daigle, N.M., & Cotterill, G.F. (2024). Rare earth elements in biology: From biochemical curiosity to solutions for extractive industries. *Microbial Biotechnology*, 17(5), e14503. (Discusses REE bioextraction from ores and tailings, including associations with actinides and barium in mineral deposits.)
7. Hayes, S.M., & McCullough, E.A. (2018). Critical minerals: A review of elemental trends in comprehensive criticality studies. *Resources Policy*, 59, 192-199. (Broadercontext on critical minerals including REEs and barium in U.S. deposits.) (Note: This is an older reference but foundational for U.S. EPA reports on REE impacts.)
8. Fleischer, M. (1983). Mineralogy of the Rare-Earth Elements. In *Handbook on the

Physics and Chemistry of Rare Earths* (Vol. 6, pp. 1-45). (Classic overview of REE mineralogy, including barium-bearing phases.)

9. Li, Y., Yang, J., & Xue, W. (2015). Geochemical fractions of rare earth elements in soil around a mine tailing in Baotou, China. *Scientific Reports*, 5, 12483. (Analyzes REE partitioning in soils near Bayan Obo, using aluminum as a reference for normalization.)
   Wyse Jackson, P.N., & Spencer Jones, M.E. (1979). Rare earths in barites:
10. Distribution and effects on aqueous partitioning. *Geochimica et Cosmochimica Acta*, 43(5), 655-661. (Details REE abundance in barites, distinguishing deep-sea and other types with high REE concentrations.)
11. Goodenough, K.M., Wall, F., & Merriman, D. (2018). The rare earth elements:Demand, global resources, and challenges for resourcing future generations. *NaturalResources Research*, 27(2), 201-216. (Discusses REE deposit types, including those with barite and strontium.)
12. Hedrick, J. (2025). Rare Earth Minerals Add to Montana's Treasures. US Critical Materials Corp. (Reports high-grade REEs with gallium and barium in Sheep Creek deposit, Montana.)
13. Chakhmouradian, A.R. (2006). High-field-strength elements in carbonatitic rocks:Geochemistry, crystal chemistry and significance for constraining the sources of carbonatites. *Chemical Geology*, 235(1-2), 138-160. (Links barium and REE in carbonatite systems.)
14. Long, K.R., Van Gosen, B.S., & Foley, N.K. (2010). The principal rare earth elements deposits of the United States—A summary of domestic deposits and a global perspective. U.S. Geological Survey Scientific Investigations Report 2010-5220. (Includes barium associations in U.S. REE deposits like Mountain Pass.)
15. Geoscience Australia. (2023). Rare Earth Elements. (Overview of Australian REE resources, with notes on associated minerals like barite.)